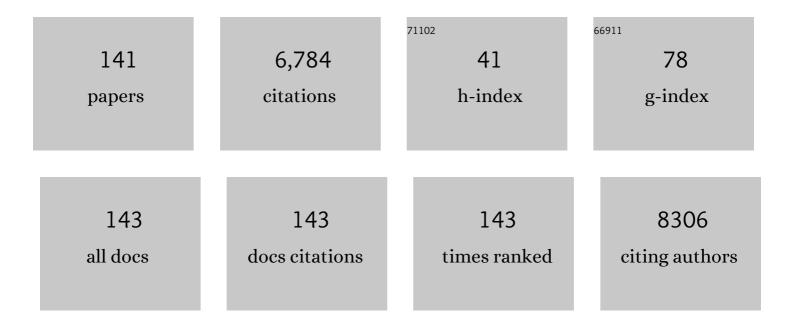
List of Publications by Year in descending order

Source: https://exaly.com/author-pdf/1889010/publications.pdf Version: 2024-02-01



#	Article	IF	CITATIONS
1	Effect of Molecular Weight on the Mechanical and Electrical Properties of Block Copolymer Electrolytes. Macromolecules, 2007, 40, 4578-4585.	4.8	449
2	Zwitterionic Polymerization of Lactide to Cyclic Poly(Lactide) by Using N-Heterocyclic Carbene Organocatalysts. Angewandte Chemie - International Edition, 2007, 46, 2627-2630.	13.8	338
3	Effect of Molecular Weight and Salt Concentration on Conductivity of Block Copolymer Electrolytes. Macromolecules, 2009, 42, 4632-4637.	4.8	309
4	Polymer Crystallization of Partially Miscible Polythiophene/Fullerene Mixtures Controls Morphology. Macromolecules, 2011, 44, 5722-5726.	4.8	256
5	Conjugated Block Copolymer Photovoltaics with near 3% Efficiency through Microphase Separation. Nano Letters, 2013, 13, 2957-2963.	9.1	253
6	Effect of Ion Distribution on Conductivity of Block Copolymer Electrolytes. Nano Letters, 2009, 9, 1212-1216.	9.1	228
7	Increased Water Retention in Polymer Electrolyte Membranes at Elevated Temperatures Assisted by Capillary Condensation. Nano Letters, 2007, 7, 3547-3552.	9.1	196
8	Nanoscale control of internal inhomogeneity enhances water transport in desalination membranes. Science, 2021, 371, 72-75.	12.6	193
9	Progress and Opportunities in the Characterization of Cellulose – An Important Regulator of Cell Wall Growth and Mechanics. Frontiers in Plant Science, 2018, 9, 1894.	3.6	155
10	Transient photovoltaic behavior of air-stable, inverted organic solar cells with solution-processed electron transport layer. Applied Physics Letters, 2009, 94, 113302.	3.3	145
11	Controlling Nucleation and Crystallization in Solutionâ€Processed Organic Semiconductors for Thinâ€Film Transistors. Advanced Materials, 2009, 21, 3605-3609.	21.0	141
12	Chain conformations and phase behavior of conjugated polymers. Soft Matter, 2017, 13, 49-67.	2.7	131
13	Glass transition temperature from the chemical structure of conjugated polymers. Nature Communications, 2020, 11, 893.	12.8	130
14	Directly patternable, highly conducting polymers for broad applications in organic electronics. Proceedings of the National Academy of Sciences of the United States of America, 2010, 107, 5712-5717.	7.1	127
15	Solvent-dependent electrical characteristics and stability of organic thin-film transistors with drop cast bis(triisopropylsilylethynyl) pentacene. Applied Physics Letters, 2008, 93, .	3.3	116
16	Sustainable Thermoplastic Elastomers Derived from Fatty Acids. Macromolecules, 2013, 46, 7202-7212.	4.8	111
17	Correlating the scattered intensities of P3HT and PCBM to the current densities of polymer solar cells. Chemical Communications, 2011, 47, 436-438.	4.1	103
18	Challenges and Opportunities in the Development of Conjugated Block Copolymers for Photovoltaics. Macromolecules, 2015, 48, 7385-7395.	4.8	103

2

#	Article	IF	CITATIONS
19	High-temperature polymers with record-high breakdown strength enabled by rationally designed chain-packing behavior in blends. Matter, 2021, 4, 2448-2459.	10.0	100
20	Effect of Miscibility and Percolation on Electron Transport in Amorphous Poly(3-Hexylthiophene)/Phenyl- <mml:math <br="" xmlns:mml="http://www.w3.org/1998/Math/MathML">display="inline"><mml:msub><mml:mi mathvariant="normal">C<mml:mn>61</mml:mn></mml:mi </mml:msub></mml:math> -Butyric Acid Methyl Ester Blends. Physical Review Letters, 2012, 108, 026601.	7.8	98
21	Azadipyrrometheneâ€Based Zn(II) Complexes as Nonplanar Conjugated Electron Acceptors for Organic Photovoltaics. Advanced Materials, 2014, 26, 6290-6294.	21.0	93
22	Correlation between Phase-Separated Domain Sizes of Active Layer and Photovoltaic Performances in All-Polymer Solar Cells. Macromolecules, 2016, 49, 5051-5058.	4.8	93
23	Influence of Acceptor Structure on Barriers to Charge Separation in Organic Photovoltaic Materials. Journal of Physical Chemistry C, 2012, 116, 4824-4831.	3.1	86
24	Predicting Chain Dimensions of Semiflexible Polymers from Dihedral Potentials. Macromolecules, 2014, 47, 6453-6461.	4.8	78
25	Glass Transition Temperature of Conjugated Polymers by Oscillatory Shear Rheometry. Macromolecules, 2017, 50, 5146-5154.	4.8	78
26	Domain Compositions and Fullerene Aggregation Govern Charge Photogeneration in Polymer/Fullerene Solar Cells. Advanced Energy Materials, 2014, 4, 1400116.	19.5	77
27	Altering the Thermodynamics of Phase Separation in Inverted Bulkâ€Heterojunction Organic Solar Cells. Advanced Materials, 2009, 21, 3110-3115.	21.0	75
28	Ceramic–Salt Composite Electrolytes from Cold Sintering. Advanced Functional Materials, 2019, 29, 1807872.	14.9	72
29	Device Characteristics of Bulk-Heterojunction Polymer Solar Cells are Independent of Interfacial Segregation of Active Layers. Chemistry of Materials, 2011, 23, 2020-2023.	6.7	71
30	Electron tomography reveals details of the internal microstructure of desalination membranes. Proceedings of the National Academy of Sciences of the United States of America, 2018, 115, 8694-8699.	7.1	69
31	Tunable Multiscale Nanoparticle Ordering by Polymer Crystallization. ACS Central Science, 2017, 3, 751-758.	11.3	60
32	Rapid fabrication of precise high-throughput filters from membrane protein nanosheets. Nature Materials, 2020, 19, 347-354.	27.5	59
33	Direct probe of the nuclear modes limiting charge mobility in molecular semiconductors. Materials Horizons, 2019, 6, 182-191.	12.2	53
34	Antibacterial Cotton Fabric Functionalized with Copper Oxide Nanoparticles. Molecules, 2020, 25, 5802.	3.8	53
35	Engineering the organic semiconductor-electrode interface in polymer solar cells. Journal of Materials Chemistry, 2010, 20, 6604.	6.7	51
36	Platelet Self-Assembly of an Amphiphilic Aâ^'Bâ^'Câ^'A Tetrablock Copolymer in Pure Water. Macromolecules, 2005, 38, 3567-3570.	4.8	48

#	Article	IF	CITATIONS
37	Catalysts from Self-Assembled Organometallic Block Copolymers. Advanced Materials, 2005, 17, 2003-2006.	21.0	45
38	Broad temperature dependence, high conductivity, and structure-property relations of cold sintering of LLZO-based composite electrolytes. Journal of the European Ceramic Society, 2020, 40, 6241-6248.	5.7	45
39	Predicting Flory-Huggins <mml:math <br="" xmlns:mml="http://www.w3.org/1998/Math/MathML">display="inline"><mml:mrow><mml:mi>l‡</mml:mi></mml:mrow></mml:math> from Simulations. Physical Review Letters, 2017, 119, 017801.	7.8	44
40	Next generation highâ€performance carbon fiber thermoplastic composites based on polyaryletherketones. Journal of Applied Polymer Science, 2017, 134, .	2.6	44
41	Predicting Nematic Phases of Semiflexible Polymers. Macromolecules, 2015, 48, 1454-1462.	4.8	43
42	Signatures of Intracrystallite and Intercrystallite Limitations of Charge Transport in Polythiophenes. Macromolecules, 2016, 49, 7359-7369.	4.8	43
43	Connecting the Mechanical and Conductive Properties of Conjugated Polymers. Advanced Electronic Materials, 2018, 4, 1700356.	5.1	41
44	Preferred crystallographic orientation of cellulose in plant primary cell walls. Nature Communications, 2020, 11, 4720.	12.8	41
45	Effect of Crystallization Kinetics on Microstructure and Charge Transport of Polythiophenes. Macromolecular Rapid Communications, 2012, 33, 2133-2137.	3.9	40
46	Characterization of the mesoscopic structure in the photoactive layer of organic solar cells: A focused review. Materials Letters, 2013, 90, 97-102.	2.6	40
47	Triplet Transfer Mediates Triplet Pair Separation during Singlet Fission in 6,13â€Bis(triisopropylsilylethynyl)â€Pentacene. Advanced Functional Materials, 2017, 27, 1703929.	14.9	40
48	Tuning Contact Recombination and Open-Circuit Voltage in Polymer Solar Cells via Self-Assembled Monolayer Adsorption at the Organic–Metal Oxide Interface. Journal of Physical Chemistry C, 2013, 117, 20474-20484.	3.1	39
49	Direct measurements of exciton diffusion length limitations on organic solar cell performance. Chemical Communications, 2012, 48, 5859.	4.1	38
50	Linking Group Influences Charge Separation and Recombination in All onjugated Block Copolymer Photovoltaics. Advanced Functional Materials, 2015, 25, 5578-5585.	14.9	38
51	Controlling Chain Conformations of Highâ€ <i>k</i> Fluoropolymer Dielectrics to Enhance Charge Mobilities in Rubrene Singleâ€Crystal Fieldâ€Effect Transistors. Advanced Materials, 2016, 28, 10095-10102.	21.0	38
52	Signatures of Multiphase Formation in the Active Layer of Organic Solar Cells from Resonant Soft X-ray Scattering. ACS Macro Letters, 2013, 2, 185-189.	4.8	37
53	Biomimetic Separation of Transport and Matrix Functions in Lamellar Block Copolymer Channel-Based Membranes. ACS Nano, 2019, 13, 8292-8302.	14.6	37
54	Synthesis of Perfluoroalkyl End-Functionalized Poly(3-hexylthiophene) and the Effect of Fluorinated End Groups on Solar Cell Performance. Macromolecules, 2013, 46, 103-112.	4.8	36

#	Article	IF	CITATIONS
55	Recent Developments in Chain-Growth Polymerizations of Conjugated Polymers. Industrial & Engineering Chemistry Research, 2017, 56, 7888-7901.	3.7	34
56	Dehydration-induced physical strains of cellulose microfibrils in plant cell walls. Carbohydrate Polymers, 2018, 197, 337-348.	10.2	34
57	New opportunities in transmission electron microscopy of polymers. Materials Science and Engineering Reports, 2020, 139, 100516.	31.8	34
58	Dispersing Grafted Nanoparticle Assemblies into Polymer Melts through Flow Fields. ACS Macro Letters, 2013, 2, 1051-1055.	4.8	32
59	Passive Parity-Time Symmetry in Organic Thin Film Waveguides. ACS Photonics, 2015, 2, 319-325.	6.6	32
60	Molecular Rectification in Conjugated Block Copolymer Photovoltaics. Journal of Physical Chemistry C, 2016, 120, 6978-6988.	3.1	32
61	Side chain length affects backbone dynamics in poly(3â€alkylthiophene)s. Journal of Polymer Science, Part B: Polymer Physics, 2018, 56, 1193-1202.	2.1	31
62	Tuning the Dielectric Properties of Organic Semiconductors via Salt Doping. Journal of Physical Chemistry B, 2013, 117, 15866-15874.	2.6	30
63	Development of a ReaxFF reactive force field for lithium ion conducting solid electrolyte Li _{1+x} Al _x Ti _{2â^'x} (PO ₄) ₃ (LATP). Physical Chemistry Chemical Physics, 2018, 20, 22134-22147.	2.8	30
64	Surface-Induced Chain Alignment of Semiflexible Polymers. Macromolecules, 2016, 49, 963-971.	4.8	29
65	Effect of Cross-Linking on the Structure and Thermodynamics of Lamellar Block Copolymers. Macromolecules, 2006, 39, 4848-4859.	4.8	27
66	Ultrathin Body Poly(3-hexylthiophene) Transistors with Improved Short-Channel Performance. ACS Applied Materials & Interfaces, 2013, 5, 2342-2346.	8.0	27
67	Resonant soft X-ray scattering reveals cellulose microfibril spacing in plant primary cell walls. Scientific Reports, 2018, 8, 12449.	3.3	26
68	Contact Doping with Subâ€Monolayers of Strong Polyelectrolytes for Organic Photovoltaics. Advanced Energy Materials, 2014, 4, 1400439.	19.5	25
69	Probing Local Electronic Transitions in Organic Semiconductors through Energyâ€Loss Spectrum Imaging in the Transmission Electron Microscope. Advanced Functional Materials, 2015, 25, 6071-6076.	14.9	25
70	Photovoltaic Performance of Block Copolymer Devices Is Independent of the Crystalline Texture in the Active Layer. Macromolecules, 2016, 49, 4599-4608.	4.8	25
71	Local Chain Alignment via Nematic Ordering Reduces Chain Entanglement in Conjugated Polymers. Macromolecules, 2018, 51, 10271-10284.	4.8	24
72	Enhancing Optoelectronic Properties of Conjugated Block Copolymers through Crystallization of Both Blocks. Macromolecules, 2020, 53, 1967-1976.	4.8	24

#	Article	IF	CITATIONS
73	The Spinning Voltage Influence on the Growth of ZnO-rGO Nanorods for Photocatalytic Degradation of Methyl Orange Dye. Catalysts, 2020, 10, 660.	3.5	23
74	Incorporating Fluorine Substitution into Conjugated Polymers for Solar Cells: Three Different Means, Same Results. Journal of Physical Chemistry C, 2017, 121, 2059-2068.	3.1	22
75	Probing the Internal Microstructure of Polyamide Thin-Film Composite Membranes Using Resonant Soft X-ray Scattering. ACS Macro Letters, 2018, 7, 927-932.	4.8	21
76	Controlling Polymorphism in Poly(3â€Hexylthiophene) through Addition of Ferrocene for Enhanced Charge Mobilities in Thinâ€Film Transistors. Advanced Functional Materials, 2015, 25, 542-551.	14.9	20
77	Mesoscopic Structural Length Scales in P3HT/PCBM Mixtures Remain Invariant for Various Processing Conditions. Chemistry of Materials, 2013, 25, 2812-2818.	6.7	19
78	Tuning the synthesis of fully conjugated block copolymers to minimize architectural heterogeneity. Journal of Materials Chemistry A, 2017, 5, 20412-20421.	10.3	19
79	Processing additive suppresses phase separation in the active layer of organic photovoltaics based on naphthalene diimide. Organic Electronics, 2014, 15, 3384-3391.	2.6	18
80	Tuning Biocompatible Block Copolymer Micelles by Varying Solvent Composition: Core/Corona Structure and Solvent Uptake. Macromolecules, 2017, 50, 4322-4334.	4.8	18
81	Fluorination of Donor–Acceptor Copolymer Active Layers Enhances Charge Mobilities in Thin-Film Transistors. ACS Macro Letters, 2017, 6, 1162-1167.	4.8	18
82	Impact of Low Molecular Weight Poly(3-hexylthiophene)s as Additives in Organic Photovoltaic Devices. ACS Applied Materials & Interfaces, 2018, 10, 2752-2761.	8.0	18
83	FIB-SEM tomography reveals the nanoscale 3D morphology of virus removal filters. Journal of Membrane Science, 2021, 640, 119766.	8.2	18
84	Polarized Soft X-ray Scattering Reveals Chain Orientation within Nanoscale Polymer Domains. Macromolecules, 2019, 52, 2803-2813.	4.8	17
85	Conjugated Block Copolymers as Model Systems to Examine Mechanisms of Charge Generation in Donor–Acceptor Materials. Advanced Functional Materials, 2019, 29, 1804858.	14.9	17
86	Pushing the limits of high-resolution polymer microscopy using antioxidants. Nature Communications, 2021, 12, 153.	12.8	17
87	Tuning of the elastic modulus of a soft polythiophene through molecular doping. Materials Horizons, 2022, 9, 433-443.	12.2	17
88	Predicting the Plateau Modulus from Molecular Parameters of Conjugated Polymers. ACS Central Science, 2022, 8, 268-274.	11.3	17
89	Nematic Order Imposes Molecular Weight Effect on Charge Transport in Conjugated Polymers. ACS Central Science, 2018, 4, 413-421.	11.3	16
90	Block Junction-Functionalized All-Conjugated Donor–Acceptor Block Copolymers. ACS Applied Materials & Interfaces, 2019, 11, 1143-1155.	8.0	16

#	Article	IF	CITATIONS
91	Signatures of the Orderâ^'Disorder Transition in Copolymers with Quenched Sequence Disorder. Macromolecules, 2004, 37, 8487-8490.	4.8	15
92	Using surface-induced ordering to probe the isotropic-to-nematic transition for semiflexible polymers. Soft Matter, 2016, 12, 6141-6147.	2.7	15
93	Creating cross-linked lamellar block copolymer supporting layers for biomimetic membranes. Faraday Discussions, 2018, 209, 179-191.	3.2	15
94	Random Copolymers Allow Control of Crystallization and Microphase Separation in Fully Conjugated Block Copolymers. Macromolecules, 2018, 51, 8844-8852.	4.8	15
95	The effect of single atom replacement on organic thin film transistors: case of thieno[3,2-b]pyrrole vs. furo[3,2-b]pyrrole. Journal of Materials Chemistry C, 2018, 6, 10050-10058.	5.5	14
96	An insight into microscopy and analytical techniques for morphological, structural, chemical, and thermal characterization of cellulose. Microscopy Research and Technique, 2022, 85, 1990-2015.	2.2	14
97	Miscibility and Acid Strength Govern Contact Doping of Organic Photovoltaics with Strong Polyelectrolytes. Macromolecules, 2015, 48, 5162-5171.	4.8	13
98	Fluoropolymer-diluted small molecule organic semiconductors with extreme thermal stability. Applied Physics Letters, 2018, 113, .	3.3	13
99	Interfacial Concentration Profiles of Rubbery Polyolefin Lamellae Determined by Quantitative Electron Microscopy. Macromolecules, 2008, 41, 156-162.	4.8	12
100	Quantifying the role of interfacial width on intermolecular charge recombination in block copolymer photovoltaics. Journal of Polymer Science, Part B: Polymer Physics, 2015, 53, 1224-1230.	2.1	12
101	Phase behavior of poly(3â€hexylthiopheneâ€2,5â€diyl). Journal of Polymer Science, Part B: Polymer Physics, 2016, 54, 1202-1206.	2.1	12
102	Revealing the Importance of Energetic and Entropic Contributions to the Driving Force for Charge Photogeneration. ACS Applied Materials & Interfaces, 2018, 10, 39933-39941.	8.0	12
103	Cold sintering to form bulk maghemite for characterization beyond magnetic properties. International Journal of Ceramic Engineering & Science, 2019, 1, 119-124.	1.2	11
104	Cold sintering process for fabrication of a high volumetric capacity Li4Ti5O12 anode. Materials Science and Engineering B: Solid-State Materials for Advanced Technology, 2019, 250, 114435.	3.5	11
105	Nanostructured Thermoset/Thermoset Blends Compatibilized with an Amphiphilic Block Copolymer. Macromolecules, 2019, 52, 3104-3114.	4.8	11
106	Molecular Weight Characterization of Conjugated Polymers Through Gel Permeation Chromatography and Static Light Scattering. ACS Applied Polymer Materials, 2021, 3, 4572-4578.	4.4	11
107	Fluorinated and hydrogenated self-assembled monolayers (SAMs) on anodes: Effects of SAM chemistry on device characteristics of polymer solar cells. Organic Electronics, 2014, 15, 3333-3340.	2.6	10
108	Resonant Soft X-Ray Scattering Provides Protein Structure with Chemical Specificity. Structure, 2018, 26, 1513-1521.e3.	3.3	10

#	Article	IF	CITATIONS
109	Imaging 0.36 nm Lattice Planes in Conjugated Polymers by Minimizing Beam Damage. Macromolecules, 2020, 53, 8296-8302.	4.8	10
110	Thioether-Based Polymeric Micelles with Fine-Tuned Oxidation Sensitivities for Chemotherapeutic Drug Delivery. Biomacromolecules, 2022, 23, 77-88.	5.4	10
111	Microstructure and Solvent Distribution in Cross-Linked Diblock Copolymer Gels. Macromolecules, 2007, 40, 5103-5110.	4.8	9
112	Controlling crystallization to improve charge mobilities in transistors based on 2,7-dioctyl[1]benzothieno[3,2-b][1]benzothiophene. Journal of Materials Chemistry C, 2015, 3, 8799-8803.	5.5	9
113	Elucidating Mechanisms for Electron Beam Damage in Conjugated Polymers. Microscopy and Microanalysis, 2018, 24, 1988-1989.	0.4	8
114	Demonstrating lowâ€ŧemperature sintering of boron carbide powders. International Journal of Ceramic Engineering & Science, 2019, 1, 178-184.	1.2	8
115	Thermal Fluctuations Lead to Cumulative Disorder and Enhance Charge Transport in Conjugated Polymers. Macromolecular Rapid Communications, 2019, 40, e1900134.	3.9	8
116	Improved Self-Assembly of P3HT with Pyrene-Functionalized Methacrylates. ACS Omega, 2021, 6, 27325-27334.	3.5	8
117	Revealing temperature-dependent polymer aggregation in solution with small-angle X-ray scattering. Journal of Materials Chemistry A, 2022, 10, 2096-2104.	10.3	8
118	Elemental Mapping of Interfacial Layers at the Cathode of Organic Solar Cells. ACS Applied Materials & Interfaces, 2014, 6, 19638-19643.	8.0	7
119	Close-Packed Spherical Morphology in an ABA Triblock Copolymer Aligned with Large-Amplitude Oscillatory Shear. Macromolecules, 2016, 49, 4875-4888.	4.8	7
120	Morphing Simulations Reveal Architecture Effects on Polymer Miscibility. Macromolecules, 2020, 53, 9386-9396.	4.8	7
121	Predicting χ of Polymer Blends Using Atomistic Morphing Simulations. Macromolecules, 2021, 54, 10447-10455.	4.8	7
122	Enhancing resistance of poly(ether ketone ketone) to highâ€ŧemperature steam through crosslinking and crystallization control. Journal of Applied Polymer Science, 2019, 136, 47727.	2.6	6
123	Aluminum oxide free-standing thin films to enable nitrogen edge soft x-ray scattering. MRS Communications, 2019, 9, 224-228.	1.8	6
124	Mechanomorphogenic Films Formed via Interfacial Assembly of Fluorinated Amino Acids. Advanced Functional Materials, 2021, 31, 2104223.	14.9	6
125	Twisted Aâ€Ðâ€A Type Acceptors with Thermallyâ€Activated Delayed Crystallization Behavior for Efficient Nonfullerene Organic Solar Cells. Advanced Energy Materials, 0, , 2103957.	19.5	6
126	Push–pull architecture eliminates chain length effects on exciton dissociation. Journal of Materials Chemistry A, 2018, 6, 22758-22767.	10.3	5

#	Article	IF	CITATIONS
127	Tuning fullerene miscibility with porphyrin-terminated P3HTs in bulk heterojunction blends. Soft Matter, 2020, 16, 9769-9779.	2.7	5
128	Connecting soft x-ray anisotropy with local order in conjugated polymers. MRS Communications, 2019, 9, 1168-1173.	1.8	4
129	Conductive triethylene glycol monomethyl ether substituted polythiophenes with high stability in the doped state. Journal of Polymer Science Part A, 2019, 57, 1079-1086.	2.3	4
130	Nematic Coupling in Polybutadiene from MD Simulations. Macromolecules, 2019, 52, 528-534.	4.8	4
131	Rapid preparation of nanodiscs for biophysical studies. Archives of Biochemistry and Biophysics, 2021, 712, 109051.	3.0	4
132	Thermoreversible Changes in Aligned and Cross-Linked Block Copolymer Melts Studied by Two Color Depolarized Light Scattering. Macromolecules, 2012, 45, 7590-7598.	4.8	3
133	Strategies for elemental mapping from energy-filtered TEM of polymeric materials. MRS Communications, 2018, 8, 1321-1327.	1.8	3
134	Resonant X-ray scattering of biological assemblies. MRS Communications, 2021, 11, 1-17.	1.8	3
135	Quantum transport in three-dimensional metalattices of platinum featuring an unprecedentedly large surface area to volume ratio. Physical Review Materials, 2020, 4, .	2.4	3
136	Atomistic level aqueous dissolution dynamics of NASICON-Type Li _{1+<i>x</i>} Al _{<i>x</i>} Ti _{2â^<i>x</i>} (PO ₄) ₃ (LATP). Physical Chemistry Chemical Physics, 2022, 24, 4125-4130.	2.8	3
137	Solar Cells: Domain Compositions and Fullerene Aggregation Govern Charge Photogeneration in Polymer/Fullerene Solar Cells (Adv. Energy Mater. 11/2014). Advanced Energy Materials, 2014, 4, .	19.5	2
138	New developments in phase Contrast Transmission Electron Microscopy with Electrostatic Phase Plate. Microscopy and Microanalysis, 2009, 15, 1086-1087.	0.4	1
139	Mechanomorphogenic Films Formed via Interfacial Assembly of Fluorinated Amino Acids (Adv. Funct.) Tj ETQq1	l 0.78431 14.9	4 rgBT /Over
140	Organic Thin-Film Transistors: Controlling Nucleation and Crystallization in Solution-Processed Organic Semiconductors for Thin-Film Transistors (Adv. Mater. 35/2009). Advanced Materials, 2009, 21, NA-NA.	21.0	0
141	Characterization of chain alignment at buried interfaces using Mueller matrix spectroscopy. MRS Communications, 2020, 10, 292-297.	1.8	0